Accepted Manuscript

Research on the B-integral Limitation of Ultra-High Peak Power Lasers

Zhaoli Li, Jie Mu, Kainan Zhou, Xiaoming Zeng, Zhaohui Wu, Xiao Wang, Xiaodong Wang, Yanlei Zuo*

National Key Laboratory of Plasma Physics, Laser Fusion Research Center, China Academy of Engineering Physics

Abstract: In the design and construction of ultra-high peak power laser systems, it is necessary to control the B-integral accumulated by the laser. But for picosecond and femtosecond lasers, there are no reasonable B-integral control standards currently. We systematically evaluate the influence of the B-integral on the output capability of picosecond and femtosecond laser systems for the first time, taking Nd:glass lasers and Ti:sapphire lasers as examples. For picosecond lasers, the compressed intensity decrease and the near-field modulation effect restrict the B-integral to aroud 1.7 and 1.9 respectively. For femtosecond lasers, the B-integral is mainly restricted by the near-field modulation effect and the far-field Strehl ratio, which limit the B-integral to 1.5 and 1.7 respectively. but the restriction made by Strehl ratio can be largely relaxed by inserting a deformable mirror. The study of the factors restricting the B-integral will provide guidance for the design of ultra-high peak power laser systems.

Keywords: B-integral, ultra-high peak power lasers, self-phase modulation, small-scale self-focusing, Strehl ratio

10.1017/hpl.2025.10033

1. Introduction

Since the advent of lasers, enhancing the laser intensity has been one of the goals pursued in the development of laser technology. Over the past few decades, thanks to the development of CPA technology [1], advanced laser gain medias, and high-power solid-state laser technologies, the peak power of laser devices has achieved a leapfrog development. Currently, several large-scale laser systems have been built or are under construction worldwide. These systems can generate laser pulses with widths as short as the picosecond and femtosecond scale, capable of delivering petawatt-level laser pulses, with a focused power density reaching 10^{22} W/cm^2 level. Such high laser power density can create unprecedented extreme physical conditions in the laboratory, providing a technical foundation and tools for many cutting-edge scientific researches, thus giving birth to the new field of strong-field physics and many interdisciplinary studies, which have become a hot topic of widespread attention and active exploration in the international academic community.

From the perspective of technical characteristics and application backgrounds, the development of ultra-intense laser technology has formed two main branches. One is the high-energy picosecond pulse laser with neodymium glass as the amplification medium, and the other is the high-peak-power femtosecond pulse laser with titanium-doped sapphire as the amplification medium. The former is mainly aimed at the research needs in fields such as laser fusion, high-energy-density physics, and materials science, while the latter is suitable for the study of strong-field physics and other fields with faster time processes. In the field of high-energy picosecond pulse lasers, the Lawrence Livermore National Laboratory (LLNL) built the world's first picosecond petawatt laser device, named Petawatt [2], in May 1996, driven by the demand for ICF ignition research. In the following decades, several picosecond petawatt laser devices such as Vulcan [3], Gekko-XII [4], NIF-ARC [5], Texas Petawatt Laser [6], and PETAL [7] were successively built in various countries. The experiments conducted on these devices have greatly enriched people's understanding of laser fusion, high-energy-density physics, and other fields.

Titanium-doped sapphire has a gain bandwidth of 230 nm, a saturation flux of 1 J/cm^2, and a high thermal conductivity, making it an ideal medium for high-peak-power, high-repetition-rate femtosecond laser pulse. The BELLA device built in Berkeley in 2013 is the world's first petawatt laser based on titanium sapphire [8]. After amplification through multiple CPA amplifiers and Ti:Sa amplifiers, this device can output a single pulse energy of >40 J, with a pulse width of less than 30 fs, a peak power of 1.3 PW, and a repetition rate of 1 Hz. Since then many Ti:Sapphire laser systems such as CoReLS [9], SULF [10], HPLS [11] were built worldwide. In addition, based on the full-chain OPCPA scheme, the Laser Fusion Research Center of China Academy of Engineering Physics successfully developed the SILEX-II device in 2017 [12], which can produce a laser pulse of 91.1 J and 18.6 fs, with a peak power of 4.9 PW. Currently, many countries and organizations are striving towards the goal of 100 PW lasers [13].

In the design and construction of ultra-short and ultra-intense laser systems, the control of B-integral is a key factor that needs to be considered. In the time domain, the introduction of B-integral leads to the generation of high-order phase distortions, which affects the compression effect of the compression grating on the laser system, resulting in a decrease in the peak intensity of the laser pulse and an increase in the pulse width after compression. In the spatial domain, on the one hand, the introduction of B-integral causes different wavefront phase distortions at

https://doi.org/10.1017/hpl.2025.10033 Published online by Cambridge University Press

different spatial positions of the laser pulse, thereby affecting the far-field focusing ability of the laser pulse; on the other hand, the small-scale self-focusing effect (SSSF) whose growth rate is proportional to the B-integral amplifies the spatial modulation in the near-field of the laser pulse, leading to a decrease in beam quality or even damage of optical elements. For high-energy nanosecond laser systems, experience suggests that the B-integral should be controlled within 2-4 [14][15]. In the NIF facility, the B-integral of one-stage amplification is controlled to be less than 1.8, and the total cumulative B-integral of all stages is controlled to be less than 3.5 [16]. At the same time, deformable mirrors, spatial filters, and other methods are used to suppress the phase and amplitude modulation in the laser pulse to improve beam quality. For broadband laser systems, some researchers suggested that the B-integral should be controlled to far less than 1 [17], but there is currently a lack systematic research on rigorous B-Integral criterion. In this paper, we calculate the changes in the compression capability, the near-field modulation, and the focusing ability of chirped laser pulse under the influence of different B-integrals, and based on this, provide a strict criterion for B-integral. Section 2 discuss the impact of the B-Integral on compression ability of chirped lasers. Section 3 discuss the near-field modulation caused by small-scale self-focusing effect related to the B-integral. Section 4 discuss the influence of the B-Integral on the laser focusing capability. Section 5 is the conclusion.

2. The impact of B-integral on the compression ability of chirped lasers

Ultra-high peak power lasers are typically generated through CPA/OPCPA technology. In this process, a low-energy broadband seed pulse is first stretched into a nanosecond pulse by a stretcher. Subsequently, the nanosecond pulse is amplified through several pieces of gain mediums or parametric crystals, and then compressed to its minimum pulse width using a compressor. During this process, the nanosecond laser pulse with a certain chirp passes through multiple transmission elements. Each time it passes through a transmission element, a nonlinear phase shift accumulates due to the nonlinear refractive index of the transmission medium, which is given by the B-integral $B = \sum \omega_0 n_2 I_0 L/c$, where ω_0 is the laser frequency, c is the speed of light, I_0 is the laser intensity, n_2 is the nonlinear refractive index of the medium, and L is the length of the medium. Since this nonlinear phase shift is related to the intensity, the local frequency at each position of the laser pulse will change, new frequency elements will be generated, which is known as self-phase modulation (SPM). SPM disrupts the linear chirp of the laser pulse, generating higher-order dispersion, making the compressor impossible to compress the laser to its minimum pulse width. Therefore, in short-pulse laser systems, considering the impact of spectral phase, it is necessary to control the B-integral accumulated during the amplification process of the laser pulse.

Assuming that the laser pulse has a certain chirp after passing through the stretcher and a B-integral of B is introduced during the amplification process, then before entering the compressor, the temporal waveform of the laser can be written as:

$$E(t) = E_0 \exp\left(-(1+iC)\frac{t^2}{2T_p^2} + iB\exp\left(-\frac{t^2}{T_p^2}\right)\right) \quad (1)$$

Here, E_0 represents the peak laser intensity, C is the coefficient of the chirp rate, $T_p = T_h/\sqrt{4\ln 2}$ is the 1/e pulse width of the chirped laser intensity, and T_h is the full width at half maximum of the laser intensity. The relationship between T_h and C is: $\Delta\omega T_h/2\pi = 0.441\sqrt{1+C^2}$, where $\Delta\omega = 2\pi c\Delta\lambda/\lambda_0^2$ is the spectral width (full width at half maximum) of the laser pulse, $\lambda_0 = 2\pi c/\omega_0$ is the central wavelength of the laser, and Δλ is the bandwidth (full width at half maximum) of the

https://doi.org/10.1017/hpl.2025.10033 Published online by Cambridge University Press

laser. In experiments, a more commonly used quantity is the chirp amount D, which is defined as the ratio of the laser's full width at half maximum to its bandwidth: $D = T_h/\Delta\lambda = 0.441\sqrt{1+C^2}\lambda_0^2/c(\Delta\lambda)^2$.

Taking the derivative of the phase term, the instantaneous frequency at each position of the laser pulse is obtained as:

$$\omega = \frac{t}{T_p^2}\left(C + 2B\exp\left(-\frac{t^2}{T_p^2}\right)\right) \tag{2}$$

Performing a Taylor expansion of the B integral term in the laser waveform:

$$E(t) = E_0 e^{iB}\exp\left(-\frac{t^2}{2T_p^2} - i(C+2B)\frac{t^2}{2T_p^2} + iB\frac{t^4}{T_p^4} + \cdots\right) \tag{3}$$

Its Fourier transform is approximately given by:

$$\tilde{E}(\omega) \approx \tilde{E}_{0\omega}\exp\left(-\frac{T_p^2}{1+i(C+2B)}\frac{\omega^2}{2} + iB\frac{6T_p^4}{\left(1+i(C+2B)\right)^4}\frac{\omega^4}{24} + \cdots\right) \tag{4}$$

When the B-integral is neglected, adjusting the compression grating to compensate for the second-order dispersion $GDD = -\frac{CT_p^2}{1+C^2}$ can minimize the pulse width of the output pulse. When the intensity increases, if no additional compensation is made by moving the compression grating under a certain B-integral, the pulse width of the output pulse will be broadened at high laser energy. Considering a chirped laser pulse with a central wavelength of 1000nm, we calculated the B-integral corresponding to the decrease of the compressed laser peak intensity to 90% under different laser bandwidths and chirp amounts. We found that within a wide range of laser bandwidths and chirp amounts (Δλ=5-50nm, D=10-500ps/nm), when the B-integral reaches approximately 0.96, the laser intensity drops to 90%. It can be seen that if the grating is set at low energy and not adjustment was made at high energy (for example, in single-shot lasers), the B integral should be designed to be less than 1.

However, in experiments, we can often achieve a more ideal compression effect by fine-tuning the spacing of the compression grating to compensate for the additional second-order dispersion induced by the B-integral. We assume that the additional second-order dispersion required to compress the high-energy laser to the limit pulse width is $GDD' = \alpha B\frac{T_p^2}{1+C^2}$, where α is an adjustable parameter. The B-integral corresponding to the decrease of the compressed laser peak intensity to 90% and the corresponding α values under different laser bandwidths and chirp amounts are shown in Figure 1. It can be seen that when the laser bandwidth and chirp amount are small, the tolerable B-integral is high. When the laser bandwidth or chirp amount increases (Δλ>4nm, D>20ps/nm), the tolerable B-integral gradually drops to a fixed value of approximately 1.7, and the corresponding α value gradually stabilizes at around 0.444. It can be seen that if the second-order dispersion can be fine adjusted, it is only necessary to control the B integral to be less than 1.7.

https://doi.org/10.1017/hpl.2025.10033 Published online by Cambridge University Press

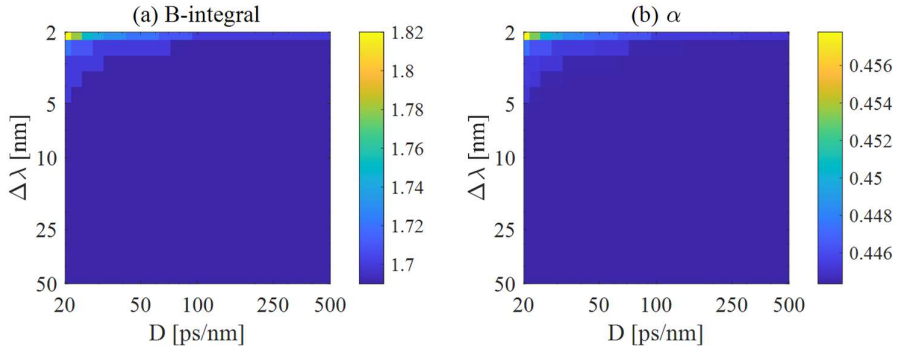

Figure 1. For Gaussian beams, (a) the maximum tolerable B-integral and (b) the corresponding α value when the laser pulse has different bandwidths and different chirp amounts.

For picosecond lasers, it is reasonable to assume that their spectrum follow a Gaussian function. However, for femtosecond lasers with broader spectral widths, the laser spectra are often shaped to approximate a rectangular distribution through spectral shaping techniques. In this case, after passing through a stretcher, the temporal waveform of the laser pulse also similar to rectangular distribution. Under such circumstances, the introduction of B-integral does not generate new frequencies in the central part of the pulse because the strength of the SPM effect is related to the gradient of the laser intensity. Therefore, the influence of the B-integral induced during the amplification process on the compressed femtosecond lasers should be weakened. To verify this, we consider a chirped laser pulse with an n_{SG} order super-Gaussian distribution in the frequency domain: $\tilde{E}(\omega) = \tilde{E}_0 \exp\left(-\frac{\ln(2)}{2}\left(2\frac{\omega-\omega_0}{\Delta\omega}\right)^{2n_{SG}} + i\frac{GDD}{2}(\omega-\omega_0)^2\right)$. First, the value of GDD is estimated using the analytical formula in Gaussian light, but this value is not applicable to super-Gaussian light. Therefore, the value of GDD needs to be finely adjusted so that the inverse Fourier transform of $\tilde{E}(\omega)$ has a specified full width at half maximum $T_h = D\Delta\lambda$ in the time domain. Then, a certain B-integral is added to the laser pulse in the time domain, and the second-order dispersion GDD' required to compress the laser to the shortest width and the corresponding laser intensity are recalculated. For a super-Gaussian laser pulse, when the laser intensity decreases to 90%, the corresponding B-integral is taken as the maximum tolerable B-integral. When the laser pulse has different bandwidths Δλ and chirp amounts D, the maximum tolerable B-integrals for n_{SG} = 2, 3, 4, and 5 are shown in Figures 2(a), (b), (c), and (d), respectively. It can be seen that for second-order super-Gaussian laser pulse, when the chirp amount and the bandwidth of the laser pulse are large enough, because the central region of the laser's temporal waveform becoming flatter, the tolerable B-integral will be much higher than that of Gaussian pulse and finally stabilize at around 5.72. However, for third-, fourth-, and fifth-order super-Gaussian pulse, the tolerable B-integral decreases to around 4.11, 3.16, and 2.83, respectively. This is because for high-order super-Gaussian pulse, the edges of the laser are steeper, and the high-order dispersions generated at the laser edges are unable to be compensated by the compressor. Therefore, a large amount of energy at the laser edges is wasted, which leads to the decrease of the maximum B-integral.

https://doi.org/10.1017/hpl.2025.10033 Published online by Cambridge University Press

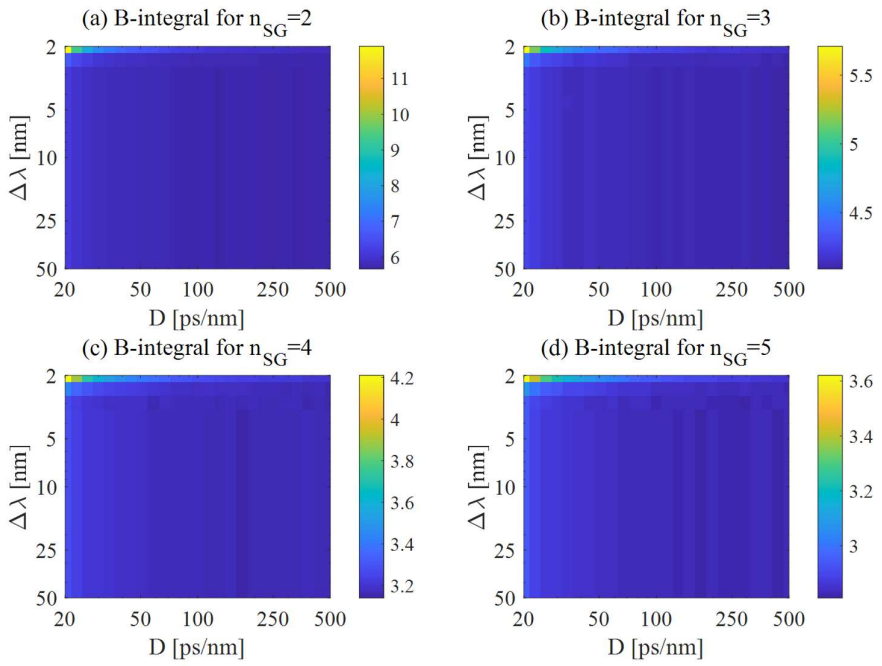

Figure 2. For super-Gaussian beams with (a) nSG = 2, (b) nSG = 3, (c) nSG = 4 and (d) nSG = 5, the maximum tolerable B-integral when the laser pulse has different bandwidths and different chirp amounts.

3. Small-scale self-focusing effect caused by the B-integral

In addition to causing high-order dispersion in the time domain, the introduction of B-integral also leads to modulation instability of the laser pulse in the spatial domain, that is, small-scale self-focusing. Small-scale self-focusing often imposes stricter requirements on the B-integral, which will be discussed through B-T theory [18]. The surface quality of optical elements can be described by the power spectral density PSD, which is defined as the square of the amplitude of the Fourier elements of the surface undulation of the element:

$$S_{ph}(k_x) = \frac{[\int z(x)\exp(-ik_x x)\,dx]^2}{\Delta k_x} \tag{5}$$

For amplitude noise, z(x) is the transmitted/reflected laser amplitude at each measurement point; for phase noise, z(x) is the measured thickness at each measurement point. Here, we only consider phase noise. For phase noise, the PSD of an optical element surface generally satisfies the following power-law relationship[19]:

$$S_{ph}(\theta) = \frac{S_0}{k_x^b} \tag{6}$$

Referring to the element parameters provided by the NIF device [20], we use the following parameters as the initial distribution of the PSD of the element surface distortion: S_0=10 [nm^2*mm]; b = 1.55, kx/2π < 1 mm^{-1}; b = 2.55, kx/2π > 1 mm^{-1}. With these parameters, the PV value of the surface distortion is 60 nm.

When an optical element introduces phase noise into a laser pulse, due to a slightly different transmission directions of noise at different spatial frequencies, the phase noise and amplitude noise of the laser will be mutually transformed during transmission in vacuum. But before the

https://doi.org/10.1017/hpl.2025.10033 Published online by Cambridge University Press

noise leaves the main laser (i.e., self-filtering [21][22][23]), the power spectrum of the noise remains unchanged. After incident on a transmission element with Kerr effect, due to the stronger laser intensity positions having a larger refractive index: $n = n_0 + n_2 I$, these positions tend to converge the surrounding beams, so the laser pulse will change from a uniform distribution to a distribution with some modulation, and the initial noise of the laser pulse will be amplified, that is, the small-scale self-focusing effect. The growth multiple of the small-scale self-focusing effect is related to the B-integral as follow:

$$G = \left(\cosh^2(\eta B) + \frac{4\Theta^2}{\eta^2}\sinh^2(\eta B)\right)\sin^2\varphi_{in} + \left(\cosh^2(\eta B) + \frac{\eta^2}{4\Theta^2}\sinh^2(\eta B)\right)\cos^2\varphi_{in} + \left(\frac{2\Theta}{\eta} + \frac{\eta}{2\Theta}\right)\cosh(\eta B)\sinh(\eta B)\sin 2\varphi_{in} \quad (7)$$

$$\Theta = \frac{n_0\theta^2}{4n_2|E_0|^2} \quad (8)$$

$$\eta = 2\sqrt{\Theta - \Theta^2} \quad (9)$$

Where $\theta = k_x/(n_0 k_0)$ is the tilt angle of the noise within the near-field, φ_{in} is the initial phase of the noise.

It can be seen that the growth rate of the small-scale self-focusing effect is related to the initial phase φ_{in} of the noise. Since the phase of the noise is usually random when it reaches the Kerr medium, the initial phase can be averaged to obtain the average growth multiple of the small-scale self-focusing effect:

$$G_{av} = 1 + \frac{2}{\eta^2}\sinh^2(\eta B) \quad (10)$$

Considering the self-filtering effect during laser transmission, that is, when the laser is transmitted in the pipe, the noise elements gradually spread out of the laser aperture and are blocked by the edge of the pipe or the downstream optical elements, resulting in a reduction of noise energy. When considering the self-filtering effect, the amplification factor of the noise should be corrected. Let the laser pulse be emitted from the source plane and then propagate freely to the target plane at a distance of L. The visible angle is defined as $\theta_v = w_0/L$, where w_0 is the radius of the laser pulse. Then, the ratio of noise between the source plane and the target plane, that is, the noise transmission rate, is given by [23]:

$$T(\theta) = \frac{2}{\pi}\int_0^1 \mathrm{Re}\left\{\arccos\left(\frac{(\theta/\theta_v)^2 + x^2 - 1}{2x\,\theta/\theta_v}\right)\right\}x dx \quad (11)$$

Therefore, the PSD of spatial noise when it reaches the target plane after starting from the noise source plane and then amplified in the Kerr medium can be expressed as:

$$S_{out}(\theta, B) = T(\theta)G_{av}(\theta, B)S_{ph}(\theta) \quad (12)$$

https://doi.org/10.1017/hpl.2025.10033 Published online by Cambridge University Press

We take the Nd:Glass laser as an example. For phosphate glass, typical parameters are n_0=1.5, n_2=3.35*10^{-20}m^2/W, and saturation energy E_s=3.1J/cm^2. After calculating the PSD of the input and output pulse, we convert the PSD back into random phase noise. Then we multiply this phase noise by a super-Gaussian distributed optical field amplitude, and let it freely propagates for a certain distance: $L_{free} = \frac{\pi c}{2\omega_0 n_2 I} \approx 1[\mathrm{m}]$, the phase noise is transformed into energy noise with a certain amplitude and phase. A simulation result with a laser intensity of 1GW/cm^2, a laser diameter of 100mm (5th order super-Gaussian distribution), a self-filtering path length of 1 meter, and a B-integral of 2, is shown in Figure 3.

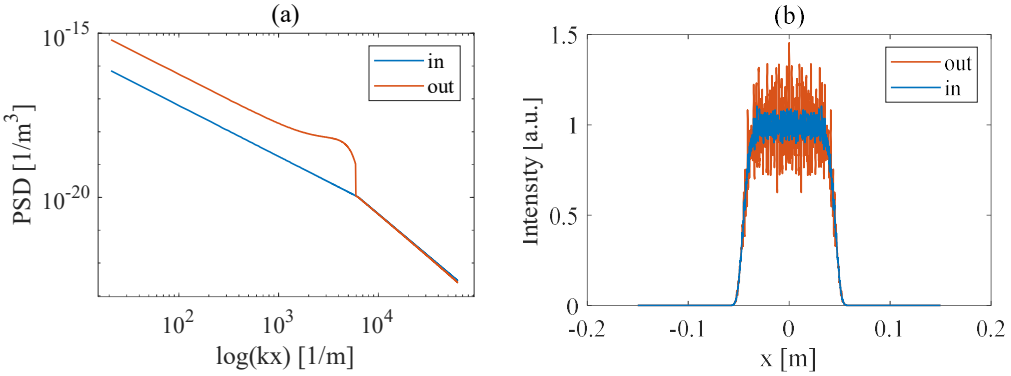

Figure 3. a simulation result of the PSD curves (a) and the intensity distribution (b) of the input pulse (blue solid line) and the output pulse (red solid line) with an laser intensity of 1 GW/cm², a laser diameter of 100 mm (5th-order super-Gaussian distribution), a B-integral of 2, and a self-filtering path length of 1 meter.

We take the PV value of the near-field modulation reaching 1.8 as the criterion to calculate the maximum allowable B-integral under different laser intensities. For each case, we conducted 100 times of simulation and took the average PV value. The calculation results are shown in Figure 4, where the blue, red, and yellow lines correspond to the self-filtering lengths of 1 meter, 10 meters, and 20 meters, respectively. Additionally, we also considered the cases where the initial noise energy was 0.25 times and 4 times the standard value, and the results are shown as the dashed and dotted lines in the figure, respectively. It can be seen that for a single standard optical element, the maximum tolerable B integral at a laser intensity of 1 GW/cm² is approximately 2.5, and it slightly increases as the laser intensity increases. Through the self-filtering effect, the maximum B integral can be increased by 0.1 to 0.3, and the higher the laser intensity, the more obvious the improvement effect of self-filtering. This is because when the laser intensity is high, the amplified noise are mainly the high-frequency elements, which are easier to be filtered out by self-filtering. When the PSD of the noise on the element surface reduces to 1/4 of the original, the maximum tolerable B integral increases to about 3.5. When the PSD of the noise on the element surface increases to 4 times the original, the maximum tolerable B integral decreases to about 1.7, and it remains basically unchanged as the laser intensity increases. In both cases, the B integral can be increased by 0.1 to 0.3 through self-filtering. It should be noted that the optical path length L required for self-filtering is related to the laser radius w_0. If the laser radius is doubled, to maintain the same viewing angle, the optical path length L also needs to be doubled to achieve the same self-filtering effect.

https://doi.org/10.1017/hpl.2025.10033 Published online by Cambridge University Press

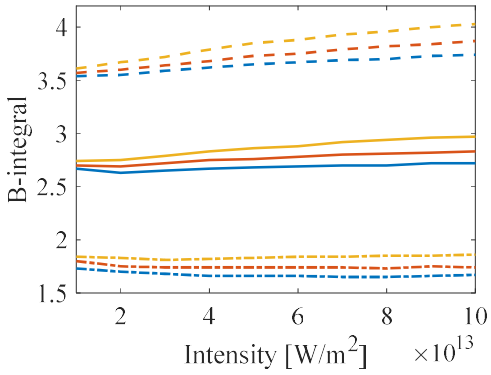

Figure 4. For rectangular-time-profile narrowband Nd:glass lasers, , the B-integral required for the near-field modulation to reach 1.8 under different initial noise energies S_0 and different self-filtering lengths L. The blue, red and yellow lines correspond to the self-filtering lengths of 1 meter, 10 meters and 20 meters respectively; the solid lines, dashed lines and dotted lines correspond to the initial noise energy being 1 time, 0.25 times and 4 times the standard value S_0 respectively.

In the above calculation, only the spatial distribution of the laser pulse was considered. The temporal distribution of the laser pulse was not considered. That is, it was assumed that the laser had a rectangular distribution in the time domain, and the chirp of the laser pulse can be neglected. With these assumptions, the amplification distribution of the spatial noise at different times are the same. Therefore, the above conclusion is only applicable to narrowband nanosecond pulses that have a rectangular distribution in the time domain. However, for picosecond lasers, although their bandwidth is relatively narrow, the laser pulse often has a Gaussian or Lorentzian distribution in the time domain. In this case, the amplification distribution of the spatial noise at different times are completely different. For femtosecond lasers, the laser pulse has different local frequencies at different times. In this case the amplification distribution of the spatial noise at different times are also different too. We first consider Nd:glass picosecond lasers, let the temporal waveform of the laser pulse be: $E(t) \propto \exp\left(-\frac{\ln(2)}{2}\left(2\frac{\omega(t)-\omega_0}{\Delta\omega}\right)^{2n_{SG}}\right)$, $\omega(t) = \frac{C}{T_p^2}t$, $\Delta\lambda = 5\text{nm}$, $n_{SG} = 1$. For each moment within the pulse width, we assume that the phase noise has the same initial distribution, and calculate the final distribution of the noise at each moment. Then we transfer the phase modulation into intensity modulation by letting the laser pulse freely propagates L_{free}. Finally, accumulate the laser intensities at each moment and calculate the near-field fluence modulation. We calculated the B-integral required for the PV value of the fluence modulation to reach 1.8 under different optical intensities, and calculated 100 times for each case and took the average value. The calculation results are shown in Figure 5, where the blue, red, and yellow lines correspond to the cases where the self-filtering length is 1 meter, 10 meters, and 20 meters, respectively. We also considered the cases where the initial noise energy is 0.25 times and 4 times the standard value, and the results are shown as the dashed and dotted lines in the figure, respectively. It can be seen that for a single standard optical element, the maximum tolerable B integral is around 2.9. When the noise energy of the element surface reduces to 1/4 of the original, the maximum tolerable B integral increases to around 3.8; When the noise energy of the element surface increases to 4 times the original, the maximum tolerable B integral decreases to around

https://doi.org/10.1017/hpl.2025.10033 Published online by Cambridge University Press

1.9. In all three cases, the tolerable B integral remains basically unchanged as the laser intensity increases. Under three self-filtering lengths, the self-filtering effect can increase the maximum B integral by 0.1 to 0.3. Although self-filtering can filter out high-spatial-frequency noise, for the characteristic optical intensity we used in the simulation, a pipe of tens of meters in length is not sufficient to effectively filter out the SSSF noise.

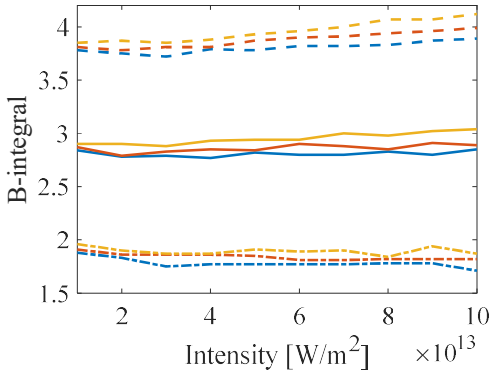

Figure 5. For picosecond Nd:glass lasers, the B-integral required for the near-field modulation to reach 1.8 under different initial noise energies S_0 and different self-filtering lengths L. The blue, red and yellow lines correspond to the self-filtering lengths of 1 meter, 10 meters and 20 meters respectively; the solid lines, dashed lines and dotted lines correspond to the initial noise energy being 1 time, 0.25 times and 4 times the standard value S_0 respectively.

Next, we consider the case of broadband femtosecond lasers. Taking the Ti:sapphire laser as an example, its specific parameters are $n_0 = 1.76$, $n_2 = 4.77\times10^{-20}$ m^2/W, and saturation energy $E_s = 0.9$ J/cm^2. For broadband lasers, although their spectrum is wide and often have a rectangular distribution, due to the different instantaneous frequencies at each moment, the SSSF at different moments also has slightly different amplification distributions. Assuming that the parameters of the femtosecond laser are $\Delta\lambda = 40\text{nm}$, $n_{SG} = 4$, and that the laser pulse has the same initial surface distortion at each moment, after the same processing as before, due to the slight difference in local wavelength at each moment, the amplification distributions of noise at different moments will be slightly different, and thus a slightly different final surface distortion will be obtained at each moment. Finally, the surface distortion is converted into wavefront phase distortion: $\varphi(x,y,t) = z(x,y,k_0(t)) \cdot k_0(t)$, and the laser pulse is allowed to freely propagate a distance L_{free}. After that the near-field fluence modulation is calculated (averaged over 100 calculations). We take the fluence modulation reaching 1.8 as the criterion and calculate the B-integral with different intensities. The calculation results are shown in Figure 6. It can be seen that for a single standard optical element, the maximum tolerable B integral in this case is about 2.5, and it slightly increases when the laser intensity increases. When the noise energy reduces to 1/4 of the original, the maximum tolerable B-integral increases to around 3.3, and it significantly increases when the laser intensity increases. When the noise energy increases to 4 times the original, the maximum tolerable B-integral decreases to around 1.5, and it remains basically unchanged when the laser intensity increases. Through the self-filtering effect, the maximum B-integral can be increased by 0.1 to 0.3, and the stronger the laser intensity, the more obvious the improvement effect of self-filtering. Overall, the calculation results of the Ti:sapphire laser in Figure 6 are not much different from those of the rectangular narrowband neodymium glass laser

https://doi.org/10.1017/hpl.2025.10033 Published online by Cambridge University Press

shown in Figure 4. Compared with narrowband lasers, broadband lasers can reduce the fluence modulation caused by SSSF through the spectral smoothing effect and thus the tolerable B-integral can be increased. However, because the wavelength of the Ti:sapphire laser is shorter than the wavelength of the Nd:glass laser, the same surface distortion of optical elements means a larger wavefront phase distortion for the Ti:sapphire laser, which offsets the benefits brought by the spectral smoothing effect. If the central wavelength of the femtosecond laser is also 1053 nm, the tolerable B-integral will be larger than the results shown here.

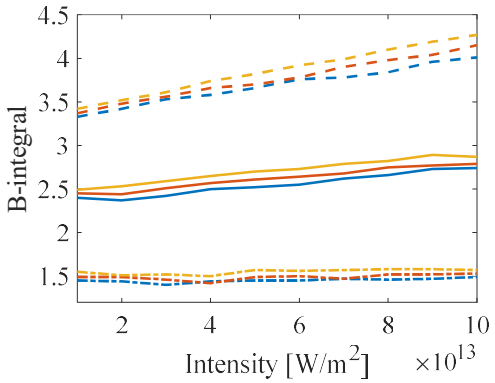

Figure 6. For femtosecond Ti:sapphire lasers, the B-integral required for the near-field modulation to reach 1.8 under different initial noise energies S_0 and different self-filtering lengths L. The blue, red and yellow lines correspond to the self-filtering lengths of 1 meter, 10 meters and 20 meters respectively; the solid lines, dashed lines and dotted lines correspond to the initial noise energy being 1 time, 0.25 times and 4 times the standard value S_0 respectively.

To evaluate the effect of the number of optical elements on the maximum allowable B-integral, we calculate the maximum allowable B-integral with different noise energies. Setting the self-filtering length to 1 meter and the laser intensity to 10^{13}W/m^2, the results for picosecond Nd:glass laser and femtosecond Ti:sapphire laser are shown by the blue and red solid lines in Figure 7, respectively. One can see that when the initial noise energy changes, the B-integral between the Nd:glass picosecond leaser and the Ti:sappihe femtosecond laser remains around 0.4, which is mainly attributed to the different tolerance degree of surface distortions between the two lasers. Due to its smaller wavelength, Ti:sapphire laser is more sensitive to surface distortion. When S0 equals 40, that is, after passing through 16 optical elements, the B-integral that the Nd:glass picosecond leaser and the Ti:sappihe femtosecond laser can tolerate are 1.88 and 1.45, respectively, as discussed above. We will use this value as the B-integral criterion to control SSSF effect.

https://doi.org/10.1017/hpl.2025.10033 Published online by Cambridge University Press

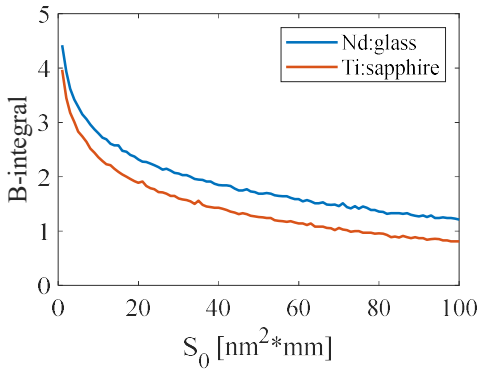

Figure 7. The maximum allowable B-integral with different noise energies. The results for picosecond Nd:glass laser and femtosecond Ti:sapphire laser are shown by the blue and red solid lines respectively.

4. The Influence of B-Integral on laser focusing capability

Other than causing SSSF effect in the near-field, the B-integral also induces wavefront phase distortion which didn't increase the intensity modulation in the near-field, but will degenerate the focal spot in the far-filed. The transmission or reflection spatial filter can suppress the growth of the laser intensity modulation in the near-field and protect the optical elements from laser damage. The wavefront phase distortion can also be compensated by a deformable mirror. However, this compensation is not perfect. On the one hand, the laser intensity varies at different moments, causing different wavefront phase distortions, while the deformable mirror can only compensate for the wavefront phase distortion at a certain moment. On the other hand, the unit size of the deformable mirror is limited, which means it can only compensate for the phase distortion in the low spatial frequency region. In this section, we use the (time-integrated) Strehl ratio of the far-field as the standard to calculate the influence of the B-integral on the laser focusing capability under different cases, and accordingly provide the B-integral criterion for broadband lasers. The specific calculation method is as follows: assume the central wavelength of the laser is 1 μm. For the amplitude noise of a laser electric field, its power spectral density (PSD) can be approximately described by the following power function relationship [19]:

$$S_a(\theta) = \frac{S_{a0}}{\theta^b} \tag{13}$$

The following parameters are used as the values of the PSD function: $S_{a0} = 1.75*10^{-6}$, b = 1.55. To simulate the filtering effect of the spatial filter, we ignore the intermediate and high frequency parts of the PSD function and generate a spatial intensity distribution using the low frequency part with a wave number less than $2\pi*0.03$ mm^{-1}. We increase the laser diameter to 300 mm (5th-order super-Gaussian distribution) to better simulate the low frequency distortion, with a step size of dx = dy = 2 mm. To better observe the influence of the B-integral on the focal spot, we do not introduce phase distortion into the laser electric field. A spatial intensity distribution generated by the above method is shown in Figure 8.

https://doi.org/10.1017/hpl.2025.10033 Published online by Cambridge University Press

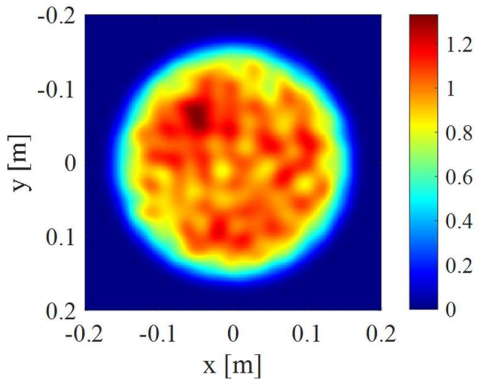

Figure 8. A spatial intensity distribution generated by the simulation program.

After generating the spatial distribution, in the time coordinate, we set the laser profile as a chirped laser pulse with an nSG-order super-Gaussian distribution. After passing through the Kerr medium, the laser accumulates a certain amount of B-integral. The laser pulse is then compressed back to the transform limit, and a phase compensation is given to the laser pulse through a deformable mirror. Theoretically, the phase to be compensated by the deformable mirror should be the phase of the compressed laser at the moment of the highest intensity, which can achieve the best compensation effect. However, in actual experiments, this phase cannot be measured. Therefore, we choose the phase distribution at the central wavelength of the laser pulse before compression as the phase to be compensated by the deformable mirror [24]. The unit sizes of the deformable mirror are 1mm, 20mm, and 30mm, respectively. For a broadband laser pulse under the paraxial approximation, the far-field fluence distribution $F_f(x_f,y_f)$ at the focal plane after passing through an ideal lens can be calculated through the Fresnel-Kirchhoff integral [24]:

$$S_0(\omega, x_0, y_0) = \frac{1}{\sqrt{2\pi}} \int E(t, x_0, y_0) e^{-i\omega t} dt \tag{14}$$

$$S_f(\omega, x_f, y_f) = \frac{-ik(\omega)}{2\pi f} e^{-ik(\omega)f - ik(\omega)\frac{x_f^2+y_f^2}{2f}} \iint S_0(\omega, x_0, y_0) e^{ik(\omega)\frac{x_0 x_f + y_0 y_f}{f}} dx_0 dy_0 \tag{15}$$

$$F_f(x_f, y_f) = \int \left| S_f(\omega, x_f, y_f) \right|^2 d\omega \tag{16}$$

The values of $F_f(0,0)$ in the far-field focal spot with a certain amount of B-integral and without B-integral are calculated respectively, and the ratio of the two is the (time-integrated) Strehl ratio. The calculation results of the Strehl ratio under different B-integrals and different deformable mirror unit sizes are shown in Figure 9. We take the Strehl ratio decreasing to 0.8 as the maximum tolerable B-integral. It can be seen that when the laser bandwidth is 5nm, 10mm, 20mm, and 40mm, the maximum tolerable B-integral without a deformable mirror is 2.2, 1.9, 1.8, and 1.7, respectively. After adding a deformable mirror with a unit size of 30mm, the maximum tolerable B-integral increases to 3.2, 3.7, 3.9, and 4, respectively. When the unit size of the deformable mirror is 20mm, the maximum tolerable B-integral further increases to 3.6, 4.7, 5.2, and 5.4, respectively. When the unit size of the deformable mirror is 10mm, the maximum tolerable B-integral is 4.4, >6, >6, and >6, respectively. If the deformable mirror is not installed, the Strehl ratio decreases more severely when the B-integral increases for wider laser bandwidths and larger n_{SG}. This is because the leading and trailing edges of broadband lasers with larger n_{SG} have higher intensities, and under the same B-integral, the leading and trailing edges accumulate larger

https://doi.org/10.1017/hpl.2025.10033 Published online by Cambridge University Press

nonlinear phase shifts, thus having more severe wavefront phase distortions. However, after adding a deformable mirror, the Strehl ratio of the laser pulse shows a significant improvement. Moreover, the wider the laser bandwidth and the larger n_{SG}, the better the correction effect of the deformable mirror. This is because before compression, the temporal profile of a broadband laser is closer to a rectangular pulse with larger n_{SG}, which enhances the correction effect of the deformable mirror. For the considered laser bandwidth range, using a deformable mirror with a unit size of 30mm can achieve a satisfactory improvement in the Strehl ratio.

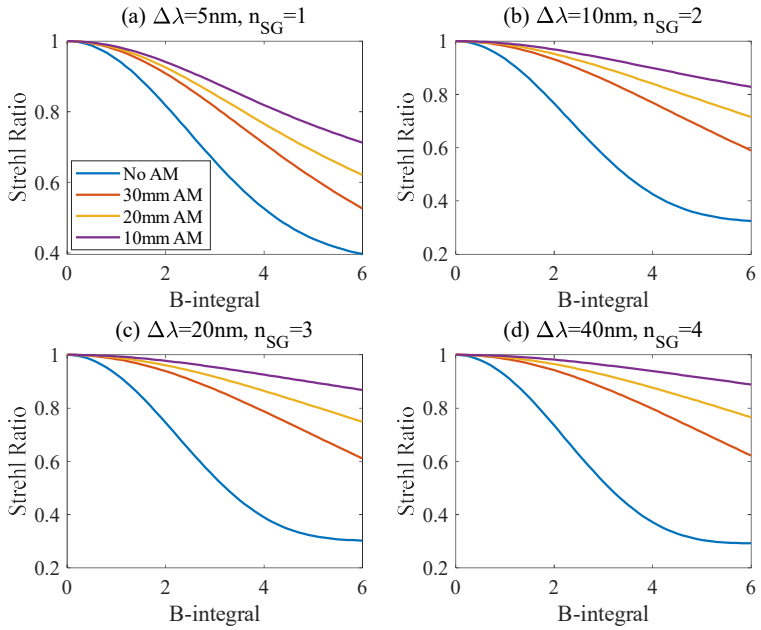

Figure 9. The variation of the Strehl ratio in the far-field with B-integral under different laser bandwidths, temporal super-Gaussian orders, and deformable mirror element sizes (no deformable mirror, 10mm, 20mm, and 30mm).

5. Conclusion

In the design and construction of ultra-high peak power laser systems, the control of B-integral has always been an important factor to consider when formulating system schemes and selecting element parameters. The influence of B-integral on ultra-high peak power lasers is mainly manifested in three aspects: in the time domain, the introduction of B-integral leads to the generation of high-order dispersion terms, affecting the compression effect of the laser pulse; in the spatial domain, on the one hand, the introduction of B-integral causes the laser pulse to have a wavefront phase distortion, thereby affecting the far-field focusing ability of the laser; on the other hand, the growth rate of the small-scale self-focusing effect in the laser pulse is directly related to the B-integral. Currently, there is no strict B-integral criterion for broadband picosecond and femtosecond lasers. The results of B-integral criterion for nanosecond lasers are usually directly applied to picosecond and femtosecond lasers, which is inappropriate. In this paper, the impact of B-integral on the output capability of broadband laser systems is evaluated using the intensity decease caused by SPM, the near-field intensity modulation caused by SSSF, and the far-field Strehl ratio as indicators. In the calculation of near-field modulation, Nd:glass lasers and

https://doi.org/10.1017/hpl.2025.10033 Published online by Cambridge University Press

Ti:sapphire lasers were taken as typical examples of picosecond and femtosecond laser systems, respectively. For picosecond lasers, the SPM effect and the SSSF effect limit the maximum tolerable B-integral. SPM limits the maximum tolerable B-integral to around 1.7, while SSSF limits the maximum tolerable B-integral to around 2. For femtosecond lasers, the amount of the B-integral is mainly limited by the SSSF effect and the far-field Strehl ratio. SSSF limits the maximum tolerable B-integral to around 1.5. If the SSSF effect is suppressed by reducing the number of optical elements or decreasing the surface distortion of the optical elements, the limitation on the B-integral can be relaxed to around 2.5. Within the studied parameters range, the self-filtering effect has a relatively small impact on the maximum B-integral, and only when the laser intensity is relatively high can the self-filtering effect significantly increase the maximum B-integral. For picosecond or femtosecond lasers, the far-field focusing ability limits the B-integral to 2.2 or 1.7, which is a strong restriction. However, this restriction can be largely relaxed by inserting a deformable mirror. It should be noted that the calculations in this paper are based on the manufacturing precision of existing large optical elements, but results hold true for a wide range of precision. The study of the B-integral will provide guidance for the design of ultra-high peak power laser systems and improvement of manufacturing precision for optical components.

Funding: This research is funded by the National Key Laboratory of Plasma Physics (6142A04220204, 6142A04230303, JCKYS2023212802, JCKYS2024212806) and the National Key Research and Development Program of China (2022YFB3606305).

Reference:

[1] D. Strickland, G. Mourou. Compression of amplified chirped optical pulses. Opt . Commun. 56, 219 (1985).
[2] M . D. Perry, D. Pennington, B. C. Staurt et al . Pettawatt laser pulses. Opt. L ett. 24, 161 (1999).
[3] C. N. Danson et al. Vulcan pettawatt: an ultra-high-intensity interaction facility. Nucl. Fusion 44, 239 (2004)]
[4] Y. Kitagawa, H. Fujita, R. Kodama. Prepulse-free petawatt laser for fast ignitor. ILE Osaka Univ. Ann. Progr. Rep. ,2002. 12-21.
[5] J. M. Di Nicola et al. The Commissioning of the Advanced Radiographic Capability Laser System: Experimental and Modeling Results at the Main Laser Output. Proc. of SPIE 9345, February 2015.
[6] E. W. GAUL et al. Demonstration of a 1.1 petawatt laser based on a hybrid optical parametric chirped pulse amplification/mixed Nd:glass amplifier[J]. Applied Optics 49, 1676 (2010),
[7] N. BLANCHOT et al. 1.15 PW-850 J compressed beam demonstration using the PETAL facility. Optics Express 25, 16957 (2017).
[8] W. P. Leemans, J. Daniels, A. Deshmukh, A. J. Gonsalves, A. Magana, H. S. Mao, D. E. Mittelberger, K. Nakamura, J. R. Riley, D. Syversrud, C. Toth, and N. Ybarrolaza, in Proceedings of PAC2013 (2013), paper THYAA1.
[9] J. H. Sung et al. 4.2 PW, 20 fs Ti:sapphire laser at 0.1 Hz. Opt. Lett. 42, 2058 (2017).
[10] Wenqi Li et al. 339 J high-energy Ti_sapphire chirped-pulse amplifier for 10 PW laser facility. Optics Letters 43, 5681 (2018).
[11] Christophe Radier et al. 10 PW peak power femtosecond laser pulses at ELI-NP. High Power

https://doi.org/10.1017/hpl.2025.10033 Published online by Cambridge University Press

Laser Science and Engineering. 10, e21 (2022).
[12] Xiaoming Zeng et al. Multi-petawatt laser facility fully based on optical parametric chirped-pulse amplification. Opt. Lett. 42, 2014 (2017).
[13] C. N. Danson et al. Petawatt and exawatt class lasers worldwide. High Power Laser Science and Engineering 7, 172 (2019).
[14] J. A. Fleck, J.R. Morris, E.S. Bliss. Small-scale self-focusing effects in a high-power glass laser amplifier. IEEE J. Quant. Elec. 14, 353–363 (1978).
[15] J. Bunkenberg, J. Boles, D.C. Brown et al. The Omega high power phosphate–glass system: design and performance. IEEE J. Quant. Elec. 17, 1620 – 1628 (1981).
[16] V. N. Ginzburg et al. FEATURES OF THE DEVELOPMENT OF THE SMALL-SCALE SELF-FOCUSING IN SUPERPOWER FEMTOSECOND LASERS. Radiophysics and Quantum Electronics 62, 849 (2020).
[17] Ian N. Ross et al. Analysis and optimization of optical parametric chirped pulse amplification. J. Opt. Soc. Am. B 19, 2945 (2002).
[18] V. I. Bespalov and V. I. Talanov. Filamentary structure of light beams in non-linear liquids. JETP Lett. 3, 307-310 (1996).
[19] V. N. Ginzburg et al. Features of the development of the small-scale self-focusing in superpower femtosecond lasers. Radiophysics and Quantum Electronics 62, 849 (2020).
[20] M. L. Spaeth et al. National Ignition Facility wavefront requirements and optical architecture. Opt. Eng. 43(12) 2854 (2004).
[21] S. Mironov et al. Suppression of small-scale self-focusing of high-intensity femtosecond radiation. Appl. Phys. B 113, 147 (2013).
[22] V. N. Ginzburg et al. Suppression of small-scale self-focusing of high-power laser beams due to their self-filtration during propagation in free space. Quantum Electron. 48 325 (2018).
[23] V. N. Ginzburg et al. Features of the Development of the Small-Scale Self-Focusing in Superpower Femtosecond Lasers. Radiophysics and Quantum Electronics 62, 849 (2020).
[24] Mikhail Martyanov et al. Improvement of the focusability of petawatt laser pulses afternonlinear post-compression. JOSAB 39, 1936 (2022).

https://doi.org/10.1017/hpl.2025.10033 Published online by Cambridge University Press